

# Fabrication and characterization of AlN/PTFE composites with low dielectric constant and high thermal stability for electronic packaging

Chen Pan<sup>1</sup> · Kaichang Kou<sup>1</sup> · Guanglei Wu<sup>1,2</sup> · Yu Zhang<sup>1</sup> · Yiqun Wang<sup>1</sup>

Received: 10 July 2015 / Accepted: 4 September 2015 / Published online: 11 September 2015  
© Springer Science+Business Media New York 2015

**Abstract** In this work, PTFE composites filled with Aluminum Nitride (AlN) were prepared by powder processing technique. The microstructure of AlN particles and the composites were investigated by scanning electron microscopic method. The effect of different weight fraction of AlN (0–0.6) on the dielectric, thermal, mechanical properties of the composites was investigated. All composites exhibited excellent thermal stability endowed by PTFE matrix. The dielectric constant and dielectric loss of the sample with 50 wt% of AlN filler was 4.2 and 0.006, at 1 MHz. The dielectric constant of the composites showed only a very small variation with frequency in the range 100–1 MHz. Several theoretical models were used to compare with experimental data of the dielectric constant of the composites. EMT model showed the best correlation with the experimental results.

## 1 Introduction

With the rapid development of the electronics industry, there has been an ever increasing demand for the high performance dielectric materials. For microelectronic packaging application, dielectric materials with suitable dielectric constant, low dielectric loss, high thermal conductivity and good thermal stability are required. At present, such materials are mainly ceramics, which have the drawbacks such as high brittleness, low dielectric strength, high processing temperature and high density. In contrast, polymers have advantages of easy processing, high flexibility, high dielectric strength and low density. Ceramic/polymer composites can combine the better aspects both of polymers and ceramics and have been seen as a group of materials which are suitable for functional and demanding electronic products [1].

The most widely used polymers are polyethylene (PE) [2], polypropylene (PP) [3], polystyrene (PS) [4] and poly methyl methacrylate (PMMA) [5, 6]. However, the thermal stability of PE, PP, PS and PMMA is low and can't run at high temperature. Compared with them, polytetrafluoroethylene (PTFE) is a kind of special engineering plastic. It has self fire-retardant, excellent chemical inertness, high operating temperature (250 °C), low water absorption and low dielectric loss tangent ( $3 \times 10^{-4}$ ) [7], which is an ideal polymer matrix for the application in the dielectric materials. However, applications are limited by high value of linear coefficient of thermal expansion. Recently, there have been many researches on the dielectric properties of PTFE composites. Particulate fillers such as SiO<sub>2</sub>, CeO<sub>2</sub>, ZnAl<sub>2</sub>O<sub>4</sub>-TiO<sub>2</sub>, MgTiO<sub>3</sub>, ZrTi<sub>2</sub>O<sub>6</sub>, Sr<sub>2</sub>ZnSi<sub>2</sub>O<sub>7</sub> and Sm<sub>2</sub>Si<sub>2</sub>O<sub>7</sub> [7–13] have been incorporated into the PTFE matrix, and their dielectric properties have been investigated. It is noteworthy that few of them involved the thermal stability

---

✉ Chen Pan  
pc@mail.nwpu.edu.cn

✉ Guanglei Wu  
wuguanglei@mail.xjtu.edu.cn

<sup>1</sup> Ministry of Education and Shanxi Key Laboratory of Macromolecular Science and Technology, School of Science, Northwestern Polytechnical University, Xi'an 710129, People's Republic of China

<sup>2</sup> State Key Laboratory of Electrical Insulation and Power Equipment, Center of Nanomaterials for Renewable Energy (CNRE), School of Electrical Engineering, Xi'an Jiaotong University, Xi'an, People's Republic of China

of PTFE composites. Thermal stability is one concern for dielectric materials, since self-generated heat and a rise in temperature during operation can lead to high losses and premature.

In order to develop suitable composites for packaging applications, the prime requirement is that the filler should have low dielectric relative permittivity, low dielectric loss, high thermal conductivity and good thermal stability. Aluminum Nitride (AlN) is a kind of well known material for dielectric application owing to high thermal conductive, low thermal expansion coefficient, high electrical resistivity and high thermal resistance. Recently, many studies [6, 14, 15] were conducted to investigate the effect of AlN on the properties of various polymer composites. Xu et al. [14] reported that the introduction of silane grafted AlN effectively enhanced the thermal stability, thermal conductivity and mechanical properties of the polyetherimide composites. Zhou et al. [6] used AlN in PMMA matrix in order to maximum the thermal conductivity and relative permittivity. The results showed that the thermal conductivity and relative permittivity of PMMA filled 0.7 vol AlN were improved to 1.87 W/(mK) and 4.4. To the best of our knowledge, the dielectric properties of AlN/PTFE composites have not been investigated. Based on such background, the AlN/PTFE composites with various filler content were prepared by cold pressing followed by sintering in the present study. The dielectric, thermal, mechanical properties of the composites were investigated. The experimental results of dielectric constant were compared with well known theoretical models including Lichtenecker equation, Jaysundere–Smith equation, Maxwell–Garnett equation and EMT equation. In addition, the microstructure and crystalline properties were studied in order to further understand the AlN/PTFE composites.

## 2 Experimental

### 2.1 Preparation of AlN/PTFE composites

PTFE powder was purchased from 3F Fluorin-chemical in Shandong Province of China. AlN powder with average size in 2  $\mu\text{m}$  was provided by Xi'an global chemical instrument company (Xi'an, China). Acetone was obtained from Xi'an chemical reagent corporation (Xi'an, China). Surfaces of AlN were modified by gamma-aminopropyl triethoxysilane (KH550), which was supplied by Jingzhou Jiangshan fine chemical Ltd (Jingzhou, China). AlN powder was dispersed in alcohol and stirred magnetically well. To the stirred suspension, calculated KH550 and deionized water were added. The amount of KH550 was 2 % of the weight of AlN powder and the amount of water was controlled exactly for the hydrolysis of KH550. The stirring

was continued for 6 h, then the slurry thus obtained was vacuum dried at 80  $^{\circ}\text{C}$  and silane modified AlN powder was obtained. The powder obtained above was weighed accurately to prepare the composites according to the weight ratio of  $x$  AlN/(1- $x$ ) PTFE ( $x = 0.1, 0.2, 0.3, 0.4, 0.5, 0.6$ ). Firstly, PTFE powder and the AlN particles were mixed by the presence of acetone. After mixing, acetone was volatilized, and then the leftover was dried at 120  $^{\circ}\text{C}$  for 2 h. Secondly, the dried powders were molded into specimen at 50 MPa for 10 min. Finally, the molded samples were heated to 375  $^{\circ}\text{C}$  at 1  $^{\circ}\text{C}/\text{min}$  and then maintained for 2 h to allow the particles coalesced completely. The cooling process was 1  $^{\circ}\text{C}/\text{min}$  from 375 to 255  $^{\circ}\text{C}$  and then cooled in the furnace [16]. The final samples were about 2 mm in thickness, 30 mm in diameter.

### 2.2 Characterization

Tensile strength of composites was tested with CMT3502 electric tension testing machine according to HG/T 2902-1997. Drawing speeding was 100 mm/min. The hardness of well polished samples was measured by Shore A durometer at a constant load of 5 kg and dwell time of 15 s. The microstructure AlN particles and the morphology of fractured cross sections of composites were examined by scanning electron microscopy (SEM, VEGA3 LMH). Samples were immersed in liquid nitrogen before rupture, and the surface were coated with about 5-nm-thick gold. DSC was performed with a TA instrument Q1000 system at a heating rate of 10  $^{\circ}\text{C}/\text{min}$  under a nitrogen atmosphere from room temperature to 380  $^{\circ}\text{C}$ . TGA analysis was performed with a TA instrument Q600ADT system at a heating rate of 10  $^{\circ}\text{C}/\text{min}$  under a nitrogen atmosphere from room temperature to 800  $^{\circ}\text{C}$ . The dielectric properties of composites were tested by using a broadband dielectric spectrometer (CONCEPE 80, Novocontrol Technology Company, Germany) with an Alpha-A high-performance frequency analyzer from 100 Hz to 1 MHz. To ensure good electrical contact, samples were evaporated with thin gold layers on both surfaces to serve as electrodes. The dielectric constant was calculated based on the measured thickness, capacitance, and the area of the electrodes.

## 3 Results and discussions

### 3.1 Microstructure of AlN particles and AlN/PTFE composites

SEM micrograph showed particulates with polygonal morphology having 0.5–5  $\mu\text{m}$ , and the mean size is about 2  $\mu\text{m}$ . With the content of AlN increases, the packing of

the particles grows denser. For the composite sample with 10 wt% AlN, almost each AlN particle is isolated and no interconnection among them is found. When the AlN content increased to 30 wt%, the particles start to connect with each other. It also can be seen that pores and voids appear in the composites, which is duo to the polymer is not enough to cover all AlN particles (Fig. 1).

### 3.2 Thermal properties and crystalline properties of AlN/PTFE composites

Melting behavior of AlN/PTFE composites was evaluated by DSC. The melting temperature, and the degree of crystallinity were listed in Table 1. The degree of crystallinity  $X_c$  was measured by the ratio of the measured fusion heat,  $\Delta H_m$  to that of a 100 % crystalline PTFE,  $\Delta H_m^\infty$  ( $69 \text{ J g}^{-1}$ ) [17]:

$$X_c = \frac{\Delta H_m}{\Delta H_m^\infty(1 - \alpha)} \quad (1)$$

where  $\alpha$  was the weight fraction of AlN in the composites. It can be seen that the filler has no significant effect on the melting points of composites. Melting points of all the composites are approximately 330 °C. Besides, there is no significant difference between these curves. It can be seen that the  $X_c$  of PTFE component in the composites is dependent on the amount of AlN. The calculated  $X_c$  of PTFE component in the composites increases from 31.6 % with increasing AlN loading from 0 to 30 wt%. However, the  $X_c$  decreases to 46.2 % with a further increase of AlN to 60 wt%. It can be interpreted by the nucleating effect of AlN for the chains of PTFE during the crystallization process. But the AlN particles start to obstruct the mobility of the PTFE chains when its loading exceeds 30 wt%. The  $X_c$  of all composites is higher than that of pure PTFE, which indicates the nucleating effect is predominant during the crystallization process (Figs. 2 and 3).

The thermal stability of AlN/PTFE composites was evaluated by TGA. The thermal decomposition

**Fig. 1** SEM micrographs of **a** AlN particles and the cross-section of AlN/PTFE composites of **b** 10 wt%, **c** 30 wt%, and **d** 60 wt%

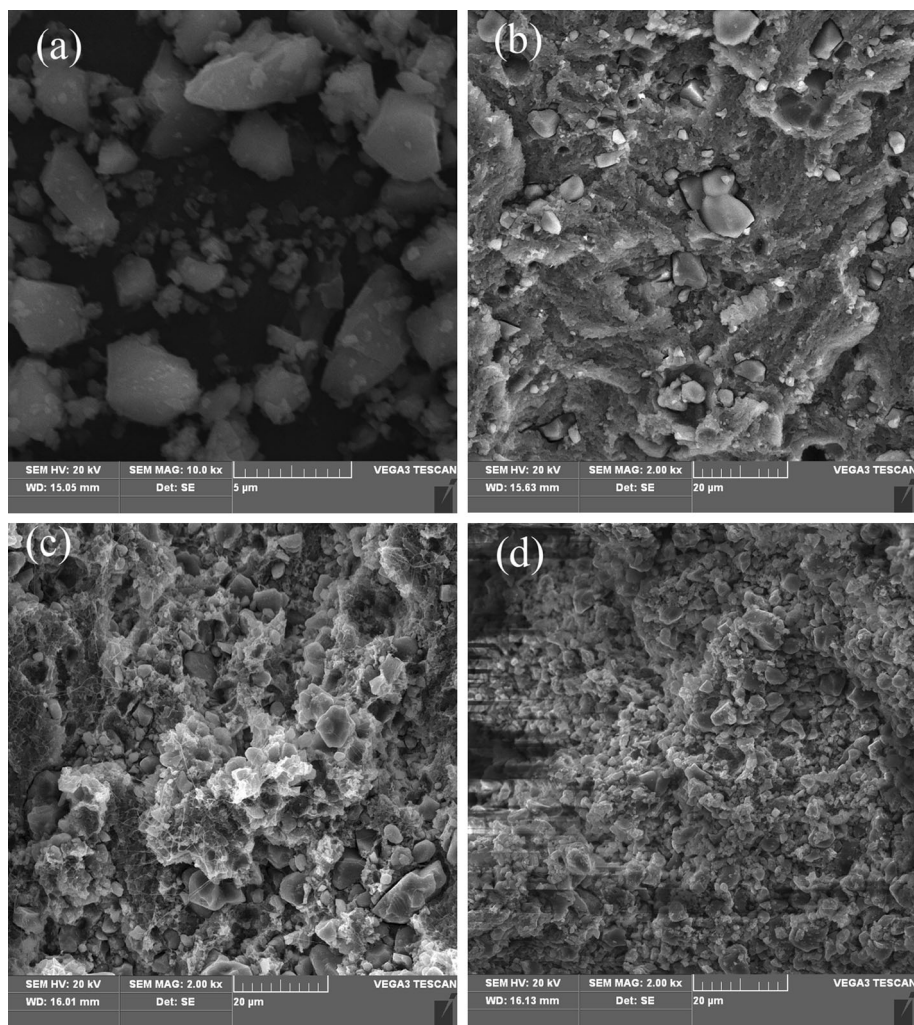


**Table 1** Melting temperature,  $T_m$ , degree of crystallinity,  $X_c$  and weight loss temperatures for the neat PTFE and the PTFE composites

AlN content (wt%)	0	10	20	30	40	50	60
$T_m$ (°C)	329.7	329.9	329.8	330.0	329.7	329.8	329.6
$X_c$ (%)	31.6	43.0	53.6	55.8	54.6	47.4	46.2
$T_{d10}$ (°C)	521.9	548.7	546.9	547.2	550.1	549.2	553.5

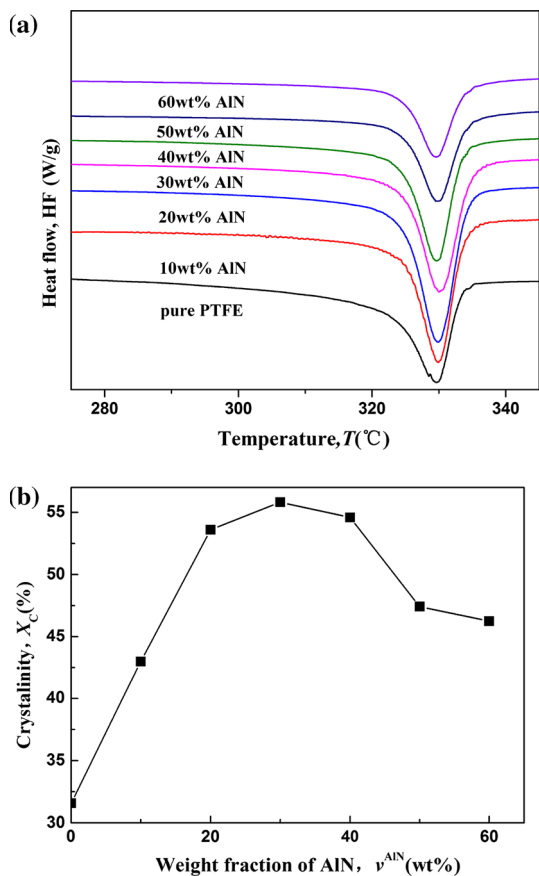


**Fig. 2** a DSC traces of neat PTFE and AlN/PTFE composites with various filler contents as indicated below each curve and b dependence of the  $X_c$  of the  $v^{AlN}$

temperature at 10 % of weight loss ( $T_{d10}$ ) is used to characterize the thermal stability of the polymer composites. It can be seen that the temperature has negligible effect on the stability of the composites until it reaches 500 °C, which can be attributed to the special helix structure and high binding energy of PTFE matrix. Meanwhile, all the curves display similar decomposition profiles within the measured temperature range, indicating that the introduction of AlN doesn't change the degradation mechanism of the PTFE matrix. Compared with the pristine PTFE, the  $T_{d10}$  of the composites increases with the increasing of AlN loading. Referring to data in Table 1, for example,  $T_{d10}$  of pristine PTFE is 521.9 °C, while  $T_{d10}$  of the composite with 60 wt% AlN is 553.5 °C, resulting in increment of 31.6 °C. The enhancement of thermal

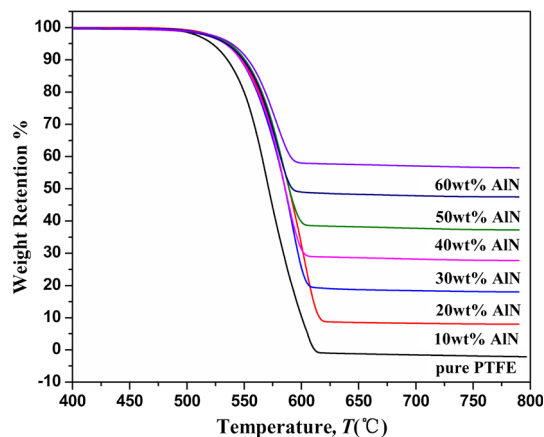


**Fig. 3** TGA curves of neat PTFE and AlN/PTFE composites with various contents as indicated below each curve

stability of the composites may be ascribed to two factors [18–20]: (1) AlN has higher thermal conductivity and higher heat capacity than PTFE, which will cause it to preferably absorb the heat. So this will result in PTFE chains starting to degrade at higher temperature; (2) the AlN filler in the composites can act as barriers, retarding the formation and volatile byproducts during pyrolysis. Meanwhile, the thermal motion of PTFE segments near the AlN surface may be restricted because of the physical interlock.

### 3.3 Mechanical properties of AlN/PTFE composites

Figure 4 showed the variation of tensile strength and shore hardness of the composites as a function of AlN content. The tensile strength of pure PTFE is relatively low because of the weak intermolecular interactions. The tensile strength of AlN/PTFE composites showed a decreasing trend with increasing filler content. This result is due to not only the decrease in the deformation area of the matrix upon increasing the fraction of the filler but also lack of adhesion between PTFE and AlN. In addition, the AlN fillers with low aspect ratio are generally not able to support stresses transferred from the polymer, and thus weaken the composites [10].

Results on the variation of shore hardness of the composites as a function of AlN content are also shown in Fig. 4. In the texturing process, there is a wide variation in the values of hardness in the case of the composites



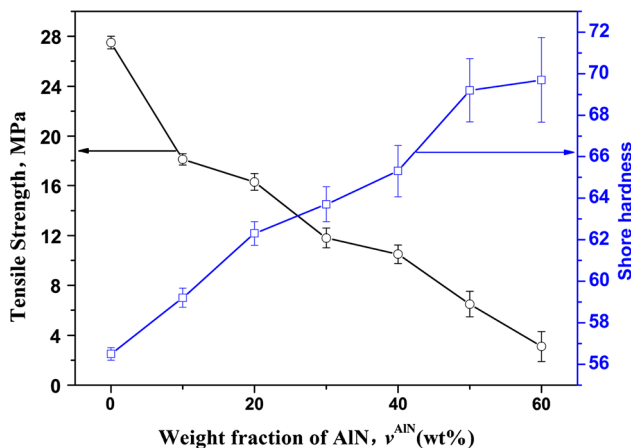


Fig. 4 Shore hardness and tensile strength of AlN/PTFE composites

containing higher content of AlN. This is probably due to the aggregation of AlN particles. To increase the accuracy of the data, an average of more than six reading was taken. It can be seen that the hardness of AlN/PTFE composites increased with increasing AlN content monotonously, which is due to the resistance to the plastic deformation of the PTFE matrix from hard AlN particles [5]. However, it also can be seen that the hardness of the composite with the filler loading at 60 wt% is little higher than the composite filled by 50 wt% AlN. This may be attributed to the presence of voids inside the composite [21].

### 3.4 Frequency dependence of dielectric properties of AlN/PTFE composites

According to Fig. 5a, it can be seen that the dielectric constant of composites with filler content up to 50 wt% remain nearly a constant in the frequency range from 1000 Hz to 1 MHz. This shows the excellent frequency stability of composites. As the filler content increases from 0 to 50 wt%, there is a gradual increase in the dielectric constant, which is due to the higher dielectric constant of AlN and the fact that dipole–dipole interaction within the powders becomes enhanced. And the lower dielectric constant of the composites compared to pure AlN may be attributed to the connectivity and the particle size effect. Moreover, the non-polar nature of PTFE matrix and the polymer molecular chains hinder the contribution of electrical polarization in the composites [22]. But the dielectric constant decreases when the content of AlN exceeds 50 wt%. The decrease of dielectric constant may be ascribed to more air voids would be involved when more filler particles were incorporated.

It is evident from Fig. 5b that the dielectric loss of the composites increases slowly with increasing in filler content from 0 to 60 wt% and the dielectric loss of all the

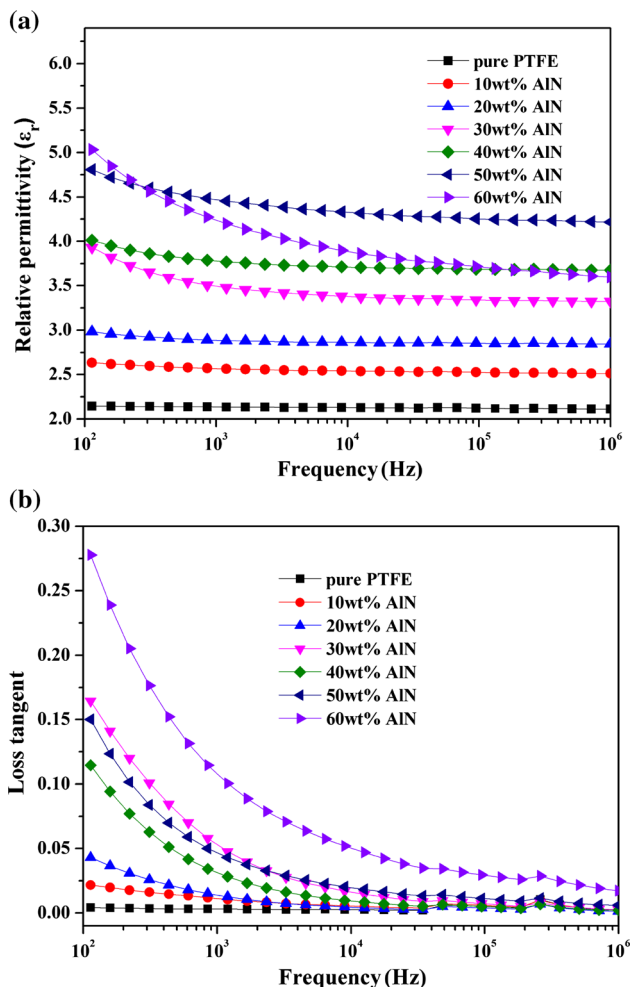


Fig. 5 Frequency dependence of a relative permittivity and b loss tangent of AlN/PTFE composites with various filler contents at room temperature

composites is blow 0.05 at the frequency from 10 kHz to 1 MHz. It is also noted that as the frequency decreases there is a gradual rise in the loss tangent for each composite, especially the composite filled by 60 wt% AlN. This can be explained based on the interfacial polarization (namely, Maxwell–Wagner effect), which would appear when the following inequality exists [23]:

$$\epsilon_{PTFE}\sigma_{AlN} \neq \epsilon_{AlN}\sigma_{PTFE} \tag{2}$$

where  $\epsilon_{PTFE}$  and  $\epsilon_{AlN}$  are the dielectric constant of PTFE and AlN particles, while  $\sigma_{AlN}$  and  $\sigma_{PTFE}$  are the conductivities of PTFE and AlN particles, respectively. Because of difference in the dielectric constant and the conductivity of the matrix and the filler, there is plentiful of accumulation of interfacial charges inside the composites under the applied electric field. As the filler content increases, the interfacial area inside the composites increases gradually and there is a gradual enhancement in the interfacial

polarization. Moreover, as the frequency is raised, the interfacial dipoles have less time to orient themselves in the direction of the alternating field [12]. As a result, as the filler content increases, the dielectric properties of the composites are more and more dependent on the frequency.

### 3.5 Theoretical prediction of AlN/PTFE composites

It is very important to predict the dielectric constant of the composites for explanation the mechanism of dielectric properties and practical applications. The dielectric properties of the composites are influenced not only by the relative permittivity of each component but also by other factors such as microstructure, dispersion and the interaction between the matrix and the filler [24]. The following equations are used to predict the dielectric permittivity of the composites: EMT model:

$$\epsilon_{eff} = \epsilon_m \left[ 1 + \frac{v(\epsilon_f - \epsilon_m)}{\epsilon_m + n(1-v)(\epsilon_f - \epsilon_m)} \right] \tag{3}$$

Lichtenecker model:

$$\log \epsilon_{eff} = v \log \epsilon_f + (1 - v) \log \epsilon_m \tag{4}$$

Jaysundere–Smith model:

$$\epsilon_{eff} = \frac{\epsilon_m(1 - v) + \epsilon_f v \left[ \frac{3\epsilon_m}{\epsilon_f + 2\epsilon_m} \right] \left[ 1 + \left( \frac{3v(\epsilon_f - \epsilon_m)}{\epsilon_f + 2\epsilon_m} \right) \right]}{1 - v + v \left[ \frac{3\epsilon_m}{\epsilon_f + 2\epsilon_m} \right] \left[ 1 + \left( \frac{3v(\epsilon_f - \epsilon_m)}{\epsilon_f + 2\epsilon_m} \right) \right]} \tag{5}$$

Maxwell–Garnett model:

$$\epsilon_{eff} = \epsilon_m \left( 1 + \frac{3v(\epsilon_f - \epsilon_m)}{2\epsilon_m + \epsilon_f - v(\epsilon_f - \epsilon_m)} \right) \tag{6}$$

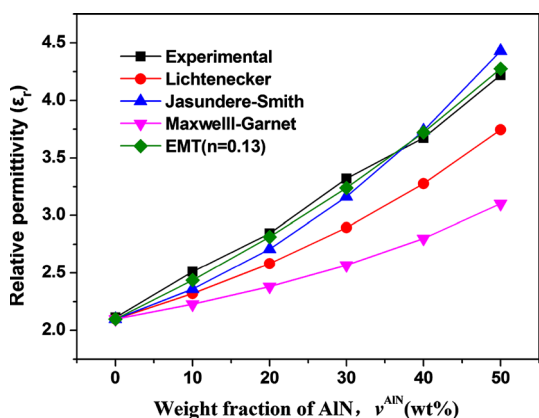
where  $\epsilon_{eff}$ ,  $\epsilon_f$  and  $\epsilon_m$  are the relative permittivity of the composites, AlN and the polymer matrix, respectively,  $v$  is the volume fraction of AlN.

Figure 6 shows the experimental values and the date predicted by equations above. It can be seen that the values predicted by Lichtenecker model and Maxwell–Garnett model have big deviations with experimental values, indicating that these two models are not suitable to describe the dielectric properties of AlN/PTFE composites. This is due to Maxwell–Garnett model suggests that filler particles should be homogeneous distributed, roughly spherical and non-interacting [25]. But in a real case, as the amount of AlN particles into PTFE increases, the interparticle distance decreases and more interfaces are introduced into the composites. The interaction between AlN particles (dipole–dipole interaction) and the interaction between AlN and PTFE (interfacial polarization) become apparent and can not be ignored. Lichtenecker model also does not consider the interphase interaction between the matrix and the filler and it is only valid in the case that the matrix and the filler have close value of dielectric constant [26]. Compared to Jaysundere–Smith model, EMT model fits better with experimental values. This can be ascribed to that Jaysundere–Smith model doesn’t consider the shape of filler [27]. For the EMT model,  $n$  is the correction factor to compensate for the shape of the fillers used in polymer composites. A small value of  $n$  indicates a near spherical shape for the filler, while a high value of  $n$  shows a largely non-spherically shaped particle. The value of the morphology fitting factor  $n$  (0.13) obtained from the fitting is a little higher than reported previously [28], which is due to the polygonal morphology of AlN.

### 4 Conclusions

PTFE composites containing 0–60 wt% AlN were prepared by powder processing technique. As the content of filler increased, the hardness of composites increased and the tensile strength decreased. The obtained composite with 50 wt% AlN showed a low dielectric constant of 4.2 and a low dielectric loss tangent of 0.006 at 1 MHz. In addition, the dielectric constant of the composites showed weak frequency dependence from 100 Hz to 1 MHz. Moreover, the composites possessed high thermal stability and all the composites showed 10 % weight loss temperatures above 500 °C. The dielectric properties as well as excellent thermal stability made the AlN/PTFE composites a promising application for electronic packaging. Theoretical models had been compared with experimental results, and the EMT equation was found to fit the best.

**Acknowledgments** This work was financially supported by the National Science Foundation of China (No. 51407134), China Post-doctoral Science Foundation (No. 2014M562412) and China Post-doctoral Science Special Foundation (No. 2015T81028).



**Fig. 6** Comparison of experimental and theoretically predicted dielectric constant through different modeling approaches at 1 MHz

## References

1. Z. Dang, J. Yuan, J. Zha, T. Zhou, S. Li, G. Hu, *Prog. Mater. Sci.* **57**, 660 (2012)
2. G. Subodh, V. Deepu, P. Mohanan, M.T. Sebastian, *J. Phys. D Appl. Phys.* **42**, 225501 (2009)
3. A. Agrawal, A. Satapathy, *J. Mater. Sci. Mater. Electron.* **26**, 103 (2015)
4. L. Zhang, J. Zhao, E. Huang, J. Zha, Z. Dang, *J. Appl. Polym. Sci.* **132**, 41398 (2015)
5. R.K. Goyal, S.S. Katkade, D.M. Mule, *Compos. B Eng.* **44**, 128 (2013)
6. Y. Zhou, H. Wang, L. Wang, K. Yu, Z. Lin, L. He, Y. Bai, *Mater. Sci. Eng. B* **177**, 892 (2012)
7. G. Subodh, M. Joseph, P. Mohanan, M.T. Sebastian, *J. Am. Ceram. Soc.* **90**, 3507 (2007)
8. S. Thomas, S. Raman, P. Mohanan, M.T. Sebastian, *Compos. A Appl. Sci. Manuf.* **41**, 1148 (2010)
9. T. Joseph, S. Uma, J. Philip, M.T. Sebastian, *J. Mater. Sci. Mater. Electron.* **22**, 1000 (2011)
10. Y. Chen, H. Lin, Y. Lee, *J. Polym. Res.* **10**, 247 (2003)
11. Y. Yuan, S.R. Zhang, X.H. Zhou, E.Z. Li, *Mater. Chem. Phys.* **141**, 175 (2013)
12. S. Thomas, V.N. Deepu, P. Mohanan, M.T. Sebastian, *J. Am. Ceram. Soc.* **91**, 1971 (2008)
13. P.S. Anjana, S. Uma, J. Philip, M.T. Sebastian, *J. Appl. Polym. Sci.* **118**, 751 (2010)
14. S. Wu, Y. Huang, C.M. Ma, S. Yuen, C. Teng, S. Yang, *Compos. A Appl. Sci. Manuf.* **42**, 1573 (2011)
15. M. Choudhury, S. Mohanty, S.K. Nayak, *Polym. Compos.* **34**, 1 (2013)
16. D. Zhang, K. Kou, P. Gao, M. Hou, M. Chao, *J. Polym. Res.* **19**, 9873 (2012)
17. D. Zhang, K. Kou, Y. Zhang, Q. Zhao, Z. Zheng, *J. Appl. Polym. Sci.* **130**, 3710 (2013)
18. L. Fang, W. Wu, X. Huang, J. He, P. Jiang, *Compos. Sci. Technol.* **107**, 67 (2015)
19. A.S. Luyt, J.A. Molefi, H. Krump, *Polym. Degrad. Stabil.* **91**, 1629 (2006)
20. W. Zhou, *Thermochim. Acta* **512**, 183 (2011)
21. R.K. Goyal, V.V. Madav, P.R. Pakankar, S.P. Butee, *J. Electron. Mater.* **40**, 2240 (2011)
22. G. Hu, F. Gao, J. Kong, S. Yang, Q. Zhang, Z. Liu, Y. Zhang, H. Sun, *J. Alloys Compd.* **619**, 686 (2015)
23. Z. Dang, H. Xu, H. Wang, *Appl. Phys. Lett.* **90**, 12901 (2007)
24. G. Subodh, C. Pavithran, P. Mohanan, M.T. Sebastian, *J. Eur. Ceram. Soc.* **27**, 3039 (2007)
25. Y. Su, C. Sun, W. Zhang, H. Huang, *J. Mater. Sci.* **48**, 8147 (2013)
26. B. Luo, X. Wang, Q. Zhao, L. Li, *Compos. Sci. Technol.* **112**, 1 (2015)
27. B. Luo, X. Wang, Y. Wang, L. Li, *J. Mater. Chem. A* **2**, 510 (2014)
28. B. Fan, J. Zha, D. Wang, J. Zhao, Z. Dang, *Appl. Phys. Lett.* **100**, 92903 (2012)